Accredited SINTA 2 Ranking
Decree of the Director General of Higher Education, Research, and Technology, No. 158/E/KPT/2021
Validity period from Volume 5 Number 2 of 2021 to Volume 10 Number 1 of 2026

Published online at: **http://jurnal.iaii.or.id**

JURNAL RESTI
(Rekayasa Sistem dan Teknologi Informasi)
Vol. 9 No. 2 (2025) 297 - 302 e-ISSN: 2580-0760

Deep learning with Bayesian Hyperparameter Optimization for Precise Electrocardiogram Signals Delineation

Annisa Darmawahyuni[1*], Winda Kurnia Sari[2], Nurul Afifah[3], Siti Nurmaini[4], Jordan Marcelino[5], Rendy Isdwanta[6]
[1,4,5,6]Intelligent Systems Research Group, Faculty of Computer Science, Universitas Sriwijaya, Palembang, Indonesia
[2]Department of Information System, Universitas Sriwijaya, Palembang, Indonesia
[3]Department of Computer Engineering, Universitas Sriwijaya, Palembang, Indonesia
[1]riset.annisadarmawahyuni@gmail.com, [2]windakurniasari@unsri.ac.id, [3]nurul@unsri.ac.id, [4]sitinurmaini@gmail.com

Abstract

Electrocardiography (ECG) serves as an essential risk-stratification tool to observe further treatment for cardiac abnormalities. The cardiac abnormalities are indicated by the intervals and amplitude locations in the ECG waveform. ECG delineation plays a crucial role in identifying the critical points necessary for observing cardiac abnormalities based on the characteristics and features of the waveform. In this study, we propose a deep learning approach combined with Bayesian Hyperparameter Optimization (BHO) for hyperparameter tuning to delineate the ECG signal. BHO is an optimization method utilized to determine the optimal values of an objective function. BHO allows for efficient and faster parameter search compared to conventional tuning methods, such as grid search. This method focuses on the most promising search areas in the parameter space, iteratively builds a probability model of the objective function, and then uses that model to select new points to test. The used hyperparameters of BHO contain learning rate, batch size, epoch, and total of long short-term memory layers. The study resulted in the development of 40 models, with the best model achieving a 99.285 accuracy, 94.5% sensitivity, 99.6% specificity, and 94.05% precision. The ECG delineation-based deep learning with BHO shows its excellence for localization and position of the onset, peak, and offset of ECG waveforms. The proposed model can be applied in medical applications for ECG delineation.

Keywords: bayesian optimization; deep learning; ECG delineation

How to Cite: A. Darmawahyuni, W. K. Sari, N. Afifah, Siti Nurmaini, Jordan Marcelino, and Rendy Isdwanta, "Deep learning with Bayesian Hyperparameter Optimization for Precise Electrocardiogram Signals Delineation", *J. RESTI (Rekayasa Sist. Teknol. Inf.)*, vol. 9, no. 2, pp. 297 - 302, Apr. 2025.
DOI: https://doi.org/10.29207/resti.v9i2.6171

1. Introduction

Electrocardiography (ECG) is an essential risk-stratification tool to observe cardiac abnormalities and determine further treatment options, with changes in ECG morphology serving as biomarkers for this purpose [1], [2]. Cardiologists can visually analyze the ECG tracings to identify cardiac abnormalities, such as ischemic changes in the ST segments. However, early detection and accurate diagnosis are crucial for timely treatment. Despite defined criteria, emergency physicians still encounter significant challenges in rapidly diagnosing such conditions [3]. Therefore, systematic methods to enhance ECG interpretation may have a significant impact on diagnosis [4]-[7].

The current deep learning (DL) revolution has provided us with an opportunity to be effective in medical applications [8]–[10]. With a deep learning approach, the ECG interpretation using a delineation technique is proposed. ECG signals contain three main waveforms, i.e., P-wave, QRS-complex, and T-wave [11]–[13]. ECG delineation involves identifying the localization and position of the onset, peak, and offset of these main waveforms. For example, in the case of ST-elevation myocardial infarction, the localization between QRS-offset and T-onset corresponds to ST-segment [14]–[17]. The implementation of deep learning and ECG delineation aims to identify substantial changes in ST

Received: 11-11-2024 | Accepted: 14-03-2025 | Published Online: 08-04-2025

segments in an attempt to increase monitoring precision [1].

DL is a very common approach used as a technology application in various studies because of its ability to automatically analyze complex patterns in data [18]. The application of DL will be used to improve the performance of ECG signal delineation. However, to obtain an optimal DL model, hyperparameter tuning is needed on the DL model. The more parameters are optimized, the more expensive the cost.

Hyperparameter tuning is the process of adjusting parameters in a DL model to improve its performance and produce an optimal model [19]. Hyperparameters play a key role in determining the extent to which a model can generalize to new data. Some common methods used in hyperparameter tuning involve grid search, random search, and Bayesian hyperparameter optimization (BHO).

Grid search is a simple and systematic method, but it is time-consuming and resource-intensive. This approach tests parameter combinations on a predetermined grid [20]. Although easy to implement and can find the best parameters, grid search is less efficient, especially in large parameter search spaces and this method does not utilize previous test result information. Random search overcomes the weaknesses of grid search by performing a random search across the entire parameter space [21]. Random search randomly selects parameter combinations to test. This method has advantages in the speed of parameter exploration, especially in large parameter spaces, but there is still a risk of missing optimal parameters and this method does not utilize previous test result information.

To handle the problems in the grid search and random search methods, there is another method, namely BHO. BHO is an optimization method used to find the optimal value of an objective function that is expensive to evaluate [19]. Bayesian optimization uses a probabilistic model to model the objective function. This method focuses on the most promising search areas in the parameter space, iteratively builds a probability model of the objective function, and then uses the model to select new points to test.

Therefore, the contributions of this study are: (1) propose an ECG delineation with a deep learning approach. The primary objective is to delineate the ECG morphology between the onset, peak, and offset of ECG waveforms. We segmented the ECG signal to P_{start} – P_{end}, P_{end} – QRS_{start}, QRS_{start} – R_{peak}, R_{peak} – QRS_{end}, QRS_{end} – T_{start}, T_{start} – T_{end} and T_{end} – P_{start}. A hyperparameter tuning method is required to obtain an optimal deep learning model, and (2) explore BHO. for hyperparameter tuning [19], [22]. BHO is an optimization method used to find the optimal value of an objective function. It focuses on the most promising search areas in the parameter space, iteratively builds a probability model from the objective function, and then uses the model to select new points to test [23]. BHO enables efficient and faster parameter searches compared to conventional tuning methods, such as grid search [24].

2. Research Methods

The research methodology of this study contains; (i) the data preparation of Lobachevsky University Electrocardiography Database (LUDB), (ii) the ECG denoising with discrete wavelet transforms (DWT), and (iii) conducting the deep learning architecture with BHO for hyperparameter tuning.

2.1 Data Acquisition

Lobachevsky University Electrocardiography Database (LUDB) consists of a 12-lead ECG signal with P, T waves, and QRS-complexes annotation [25]. There are 200 10-second records, which are digitized at 500 samples per second. There are annotated 16797 P-waves, 21966 QRS-complexes, and 19666 T-waves.

For this study, we have generated the ECG delineation model with only lead-II due to it contains the essential information for the ECG signal. The sample of ECG signal raw data that contains information on the onset, peak, and offset of P, T waves, and QRS complexes can be seen in Figure 1. Figure 1 represents an ECG waveform with detected key points, likely showing the onset, peak, and offset of each ECG segment, which X-axis (Nodes - Points): represents time or signal samples (likely in milliseconds or discrete steps); the Y-axis (Amplitude in mV): shows the ECG signal intensity, capturing electrical activity of the heart; blue line: represents the ECG waveform, capturing normal heart rhythm, and red dots: mark significant ECG feature points, including the P-wave, QRS complex, and T-wave.

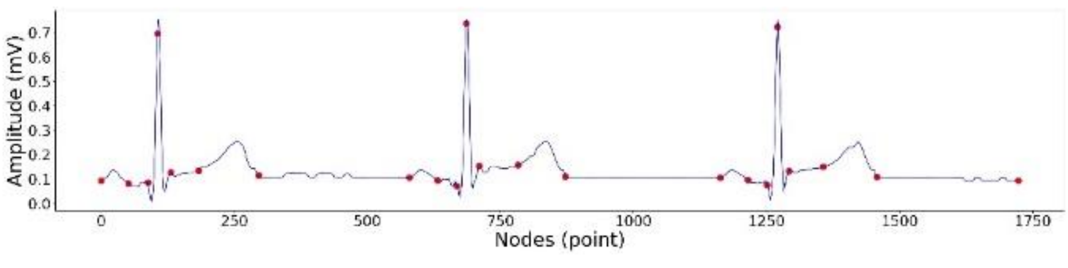

Figure 1. The sample of ECG signal with information on onset, peak, and offset of P, T waves and QRS-complexes

2.2 ECG Pre-processing

Discrete Wavelet Transform (DWT) is a signal analysis technique in the time and frequency domains. This technique is widely used to reduce noise in ECG signals [26]-[29]. The transformation process involves the use of two filters namely; low pass filter (LPF) and high pass filter (HPF). These two filters function to decompose the signal into approximate coefficients and detailed coefficients [30]. The equations of the decomposition are described in Equations 1 and 2.

$$A(k) = \sum_n x(n)h(2k-n) \quad (1)$$

$$D(k) = \sum_n x(n)g(2k-n) \quad (2)$$

$A(k)$ is approximate coefficients, $D(k)$ is detail coefficients, $h(n)$ is half band low pass filter, and $g(n)$ is a half-band high-pass filter.

After going through the decomposition process, various ECG signal processing can then be carried out, one of which is reducing noise in the signal (denoising). The denoising process involves three stages; signal decomposition, applying thresholding to detail coefficients to reduce noise in the signal, and Inverse Discrete Wavelet Transform (IDWT) or signal reconstruction. Table 1 presents 14 used mother wavelet functions, i.e., *db4, db5, db6, db7, sym5, sym8, sym10, haar, coif1, coif3, coif4, coif5,* and *bior6.8*. To find out which mother wavelet function has the best results, the signal-to-noise ratio (SNR) calculation is used. Among the experimental wavelet functions, the highest output SNR value was that of *bior6.8*, with 32.78 decibels (dB).

The bior6.8 wavelet achieved the highest SNR (32.78 dB), indicating it is the most effective at preserving signal quality while reducing noise. This makes it the most suitable candidate for ECG denoising in this study. The denoising process plays a critical role in ensuring the quality of ECG signals before waveform delineation. The decision is backed by quantitative results and is essential for improving the accuracy of downstream deep learning models.

Table 1. The used hyperparameter for BHO

Mother wavelet functions	SNR
bior6.8	32,780
db4	32,763
sym10	32,621
sym5	32,544
sym8	32,508
coif5	32,504
coif4	32,491
db6	32,482
db5	32,459
db7	32,431
coif3	32,425
coif1	31,684
haar	24,667

2.3 Deep Learning with Bayesian Hyperparameter Optimization

One-dimensional convolutional neural networks (CNNs) have one convolutional layer, with a kernel size of three with stride one. The rectified linear unit (ReLU) function was adopted with 8 filters. We have combined CNN as feature extraction and long short-term memory (LSTM) as a fully connected layer. The other hyperparameters tuning are tuned by BHO. BHO is an optimization method used to find the optimal value of an objective function that is expensive to evaluate.

BHO uses a probabilistic model to model the objective function [19]. This method focuses on the most promising search areas in the parameter space, iteratively builds a probability model from the objective function, and then uses the model to select new points to test. Based on probability models such as the Gaussian Process, BHO can understand and exploit the underlying structure of the objective function [31]. The objective function in Equation 3 represents model performance based on hyperparameter values [31].

$$f(x) = \text{Model performance (hyperparameter)} \quad (3)$$

x is hyperparameters (e.g., learning rate, batch size, number of layers), and $f(x)$ is an objective function (e.g., accuracy or loss).

This process begins with initiating a model with several starting points and then selecting the next evaluation location based on acquisition calculations, such as Expected Improvement (EI) [32]. After evaluation, the probabilistic model is updated, and this process is repeated until an optimal solution is reached. The parameters for BHO can be tuned with the following hyperparameter (refer to Table 2).

Table 2 presents the used parameters containing learning rate, batch size, epoch and total LSTM layers. The learning rate's range is well-suited for deep learning, especially for sensitive models like LSTMs or transformers. The lower bound (0.00001) allows for very fine updates, reducing the risk of overshooting the minima. Upper bound (0.001) still keeps training stable but allows faster convergence. Smaller batch sizes (8, 16) lead to noisier gradient updates, which can help escape local minima and improve generalization. Larger sizes (32) offer faster training and better use of GPU parallelism but may require more memory.

The model is trained for a minimum of 100 and up to 300 epochs. This is suitable for deep models like LSTM, especially when trained on small datasets. More epochs give room for full convergence, though they increase computational cost. The number of layers experimented with shallow to moderately deep architectures. Increasing layers may improve learning of complex features, but can also lead to vanishing gradients or overfitting with limited data.

Based on the used hyperparameter for BHO, we obtained 40 deep-learning models (refer to Table 3). Batch size 8 dominates the experiments (75%). Smaller batch sizes can improve generalization but increase training time. The presence of models with batch sizes

16 and 32 provides diversity and allows exploration of performance and computational trade-offs. Over half of the models trained for 300 epochs, suggesting the need for extended learning to reach convergence. Early stopping mechanisms might be beneficial in long training sessions to avoid overfitting. Very small learning rates (e.g., 0.00001 – 0.00007) were tested in early models (e.g., Models 3, 4, 9), which may lead to slow convergence. Higher learning rates (near 0.001) risk overshooting minima but were tested extensively (Models 11–14, 21–25).

Table 2. The used hyperparameter for BHO

Parameter	Lower Bound	Upper Bound
Learning Rate	0.00001	0.001
Batch Size	8	32
Epoch	100	300
n-layer	1	5

Table 3. The 40 deep-learning models with BHO

Model	Batch Size	Epoch	Learning Rate	Total layer
1	8	300	0.00034	3
2	16	300	0.0007	5
3	32	200	0.00007	2
4	8	300	0.00002	1
5	8	100	0.00004	2
6	32	100	0.00022	1
7	16	100	0.00003	4
8	16	200	0.00008	4
9	8	300	0.00001	5
10	32	200	0.00026	3
11	8	300	0.00075	3
12	8	300	0.00096	3
13	8	300	0.00097	4
14	8	300	0.00067	4
15	8	200	0.00047	4
16	8	300	0.00097	2
17	8	200	0.00016	2
18	8	300	0.00041	2
19	16	300	0.00046	1
20	32	200	0.0002	5
21	8	200	0.00091	2
22	8	200	0.00084	2
23	8	200	0.00051	2
24	8	300	0.00099	1
25	8	100	0.001	1
26	8	200	0.00059	1
27	8	300	0.00033	2
28	8	200	0.00058	1
29	16	300	0.00033	1
30	32	300	0.00038	3
31	8	300	0.00069	2
32	8	300	0.00071	2
33	8	300	0.00067	3
34	8	300	0.00077	2
35	8	300	0.00059	2
36	8	200	0.00084	1
37	8	300	0.00099	2
38	32	100	0.00049	1
39	16	300	0.00059	2
40	8	200	0.00029	3

3. Results and Discussions

A total of 200 records have been segmented by beat-to-beat. The total of normal beats is 1,219, which are split into 975 beats for the training set, 112 beats for the validation set, and 112 beats for the testing set (unseen). the experiments are conducted with one Intel(R) Core(TM) I9-9900K CPU @ 3.60 GHz (16 CPUs) ~3.6GHz, 32GB RAM, and one NVIDIA GeForce RTX 2080 Ti 27GB GPU (11 GB Dedicated, 16 GB Shared) is conducted. All experiments were run on Windows 10 Pro 64 Bit. We have used Python language programming with Visual Studio Code version 1.86.1 on Windows 10 Pro 64 Bit. The library is numpy, pandas, matplotlib, seaborn, wfdb, pywavelets, SciPy and TensorFlow.

The confusion matrix can be used to calculate the assessment parameters, namely; accuracy, sensitivity, specificity, precision, and F1. For the performance results of 40 models by BHO can be listed in Table 4. All presented 40 models are experimental. Among 40 models, the best performance results are achieved by model 10 with the parameters are 0.00026 learning rate, batch size of 32, 200 epochs and three hidden layers of LSTM. The performance results of model 10 achieved 99.28% accuracy, 94.5% sensitivity, 99.60% specificity, 94.05% precision, and 94.26% F1 score.

Table 4. The performance results of 40 models by BHO in the validation set

Model	Accuracy	Sensitivity	Specificity	Precision
1	99.2	93.72	99.56	93.55
2	99.17	93.78	99.54	94.02
3	99.14	92.95	99.52	93.44
4	98.92	91.84	99.4	91.73
5	99.14	93.32	99.52	93.68
6	99.03	93.08	99.46	92.8
7	99.19	93.32	99.55	93.76
8	99.21	94.13	99.56	94.11
9	99.07	91.99	99.49	92.66
10	99.28	94.5	99.6	94.05
11	99.28	94.32	99.6	94.76
12	99.31	94.45	99.62	94.53
13	99.29	94.65	99.61	94.69
14	99.26	94.64	99.59	94.4
15	99.34	95.17	99.63	94.79
16	99.31	94.65	99.62	94.99
17	99.31	94.62	99.62	94.57
18	99.3	94.91	99.62	94.47
19	99.14	93.49	99.52	93.4
20	99.27	94.12	99.59	94.29
21	99.3	94.58	99.62	94.49
22	99.15	93.49	99.53	93.89
23	76.91	12.5	87.5	0.95
24	99.22	94.16	99.57	94.01
25	99.23	94.03	99.57	94.22
26	99.18	93.86	99.54	93.95
27	99.33	94.88	99.63	94.85
28	99.28	93.93	99.6	94.68
29	99.09	93.59	99.5	92.89
30	99.26	94.27	99.59	94.61
31	99.3	94.51	99.61	94.61
32	99.28	94.48	99.6	94.47
33	99.32	94.86	99.62	94.66
34	99.3	94.46	99.61	94.54
35	97.67	83.1	98.7	83.68
36	99.14	93.13	99.53	93.45
37	99.29	94.35	99.61	94.46
38	98.94	92.99	99.42	91.86
39	99.22	94.2	99.57	93.93

For each class performance result of Model 10, the misclassification mostly occurs in P_{off}-QRS_{on} (PR-segments) with 90.29% sensitivity, 86.44% precision and 88.32% F1. The interval between atrial and ventricular activation is reflected in the PR segment. Due to their low amplitude, low frequency range, and overlap, P-waves are challenging to identify. Figure 2 shows the differences between LUDB annotated Figure 2 (a)) and ECG delineation results of $P_{start} – P_{end}$, $P_{end} – QRS_{start}$, $QRS_{start} – R_{peak}$, $R_{peak} – QRS_{end}$, $QRS_{end} – T_{start}$, $T_{start} – T_{end}$, and $T_{end} – P_{start}$ from Model 10 (Figure 2 (b)).

Figure 2 visually demonstrates the success of the ECG delineation-based deep learning model. The well-defined segmentation across multiple cycles confirms its effectiveness in waveform localization, reinforcing its suitability for medical applications. The legend on the right side provides information about the color coding: Pink (P-on - P-off): represents the P-wave region (onset to offset); orange (P-off - QRS-on): the interval between the end of P-wave and the beginning of the QRS complex; yellow (QRS-on - QRS-off): marks the QRS complex, which is the most prominent feature of an ECG; green (T-wave onset - T-wave offset): represents the T-wave, indicating ventricular repolarization; blue (Isoelectric Line): indicates the baseline (the flat line between waves). The blue dashed line represents the actual ECG waveform, showing the characteristic peaks for P-waves, QRS complexes, and T-waves.

The delineation algorithm successfully identifies the different segments of the ECG waveform. The transition points between colors align with waveform changes, meaning the algorithm correctly marks onset, peak, and offset positions. Periodic structure suggests multiple ECG cycles, indicating the model generalizes across several heartbeats. The P-wave, QRS, and T-wave segmentation is well-defined, supporting the claim that the deep learning approach effectively detects boundaries. The performance of delineation is influenced by the morphological feature of each lead. the magnitude of the shift, the direction of displacement, and the ECG segment selected for investigation all contribute to the degree of morphological changes. The difference in electrical potentials between two points in space is represented by each lead.

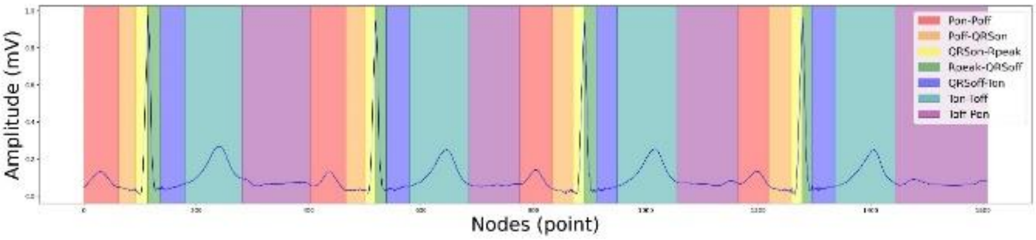

(a) LUDB annotated (ground truth)

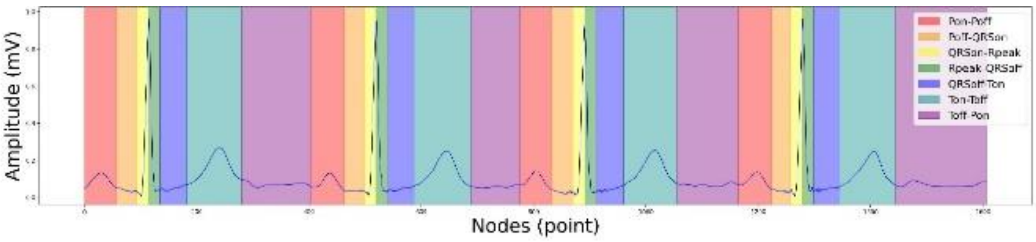

(b) DL-predicted

Figure 2. The ECG delineation results between ground truth and DL-predicted

Though the results look promising, there are limitations of this study; (1) exploring a new dataset is required, with varying frequency sampling and length of ECG records, and (2) the comparison of optimization techniques can be included in future works. The study results are based on a single dataset, meaning that model generalizability across different populations is not fully validated. The dataset might have limited variability in ECG morphology, potentially leading to bias toward specific patient groups or recording conditions. Different ECG devices record signals at different resolutions (e.g., 250 Hz, 500 Hz, 1000 Hz). The current model should be tested on multiple frequency settings to ensure robustness. Some clinical applications require long-term ECG recordings (e.g., Holter monitors) while others focus on short 10-second ECG strips. Ensuring performance across different ECG lengths is essential. Expanding to datasets with diverse cardiac conditions (e.g., arrhythmias, ischemia, and conduction blocks) will improve clinical reliability.

4. Conclusions

Precise ECG delineation is crucial for accurately identifying the onset, peak, and offset of waveform localization. ECG serves as an essential risk-stratification tool for observing further treatment for cardiac abnormalities, with changes in ECG morphology serving as biomarkers for this purpose. In this study, a deep learning approach coupled with a delineation technique is proposed for ECG interpretation. The localization and positioning of the onset, peak, and offset of the three main ECG waveforms are informed by this ECG delineation method. This study introduces an ECG delineation-based deep learning approach with BHO. As a result, 40 models were developed, with the best model achieving 99.285% accuracy, 94.5% sensitivity, 99.6% specificity, 94.05% precision, and 94.26% F1 score. The ECG delineation-based deep learning with BHO demonstrates excellence in localizing and positioning the onset, peak, and offset of P-wave, QRS-complex, and T-wave. The proposed model holds promise for application in medical contexts for ECG delineation. The integration of ECG delineation with deep learning and BHO optimization presents a powerful method for improving cardiac diagnostics. The proposed framework not only surpasses existing performance benchmarks but also lays the groundwork for real-world deployment in clinical and remote healthcare settings.

Acknowledgements

The research/publication of this article was funded by DIPA of the Public Service Agency of Universitas Sriwijaya 2024. Number of SP DIPA 023.17.2.677515/2024, On November 24, 2024. In accordance with the Rector's Decree Number:0013/UN9/LP2M.PT/2024, On May 20, 2024. We thank the Intelligent System Research Group (ISysRG), Faculty of Computer Science, Universitas Sriwijaya, Indonesia for supporting the infrastructure.

References

[1] R. Xiao *et al.*, "Monitoring significant ST changes through deep learning," *J. Electrocardiol.*, vol. 51, no. 6, pp. S78--S82, 2018.

[2] A. E. Tondas, R. A. Halim, and M. Guyanto, "Minimal or No Touch Electrocardiography Recording and Remote Heart Rhythm Monitoring during COVID-19 Pandemic Era," *Indones. J. Cardiol.*, 2020, doi: 10.30701/ijc.1010.

[3] W.-C. Liu *et al.*, "A deep learning algorithm for detecting acute myocardial infarction," *EuroIntervention*, vol. 17, no. 9, pp. 765–773, 2021.

[4] D. E. Jonas, L. C. Kahwati, J. D. Y. Yun, J. Cook Middleton, M. Coker-Schwimmer, and G. N. Asher, "Screening for atrial fibrillation with electrocardiography: Evidence report and systematic review for the US preventive services task force," *JAMA - J. Am. Med. Assoc.*, vol. 320, no. 5, pp. 485–498, 2018, doi: 10.1001/jama.2018.4190.

[5] G. Jimenez-Perez, A. Alcaine, and O. Camara, "U-Net Architecture for the Automatic Detection and Delineation of the Electrocardiogram," *Comput. Cardiol. (2010).*, vol. 2019-Septe, Sep. 2019, doi: 10.23919/CINC49843.2019.9005824.

[6] S. Nurmaini *et al.*, "Robust electrocardiogram delineation model for automatic morphological abnormality interpretation," *Sci. Rep.*, vol. 13, no. 1, p. 13736, 2023.

[7] X. Wang, Y. Jin, S. Schmitt, and M. Olhofer, "Recent advances in Bayesian optimization," *ACM Comput. Surv.*, vol. 55, no. 13s, pp. 1–36, 2023.

[8] S. Nurmaini *et al.*, "Informatics in Medicine Unlocked Electrocardiogram signal classification for automated delineation using bidirectional long short-term memory," *Informatics Med. Unlocked*, vol. 22, p. 100507, 2021, doi: 10.1016/j.imu.2020.100507.

[9] S. Nurmaini *et al.*, "Deep Learning-Based Stacked Denoising and Autoencoder for ECG Heartbeat Classification," *Electronics*, vol. 9, no. 1, p. 135, 2020, doi: 10.3390/electronics9010135.

[10] G. Sannino and G. De Pietro, "A deep learning approach for ECG-based heartbeat classification for arrhythmia detection," *Futur. Gener. Comput. Syst.*, vol. 86, pp. 446–455, 2018, doi: 10.1016/j.future.2018.03.057.

[11] A. L. Goldberger, Z. D. Goldberger, and A. Shvilkin, *Goldberger's Clinical Electrocardiography: A Simplified Approach: Ninth Edition*. 2017.

[12] S. W. Smith *et al.*, "A deep neural network for 12-lead electrocardiogram interpretation outperforms a conventional algorithm, and its physician overread, in the diagnosis of atrial fibrillation," *IJC Hear. Vasc.*, vol. 25, p. 100423, 2019, doi: 10.1016/j.ijcha.2019.100423.

[13] V. V Kuznetsov, V. A. Moskalenko, D. V Gribanov, and N. Y. Zolotykh, "Interpretable feature generation in ECG using a variational autoencoder," *Front. Genet.*, vol. 12, p. 638191, 2021.

[14] M. G. Khan, *Rapid ECG interpretation*. Springer Science & Business Media, 2008.

[15] L. Wu *et al.*, "Lasso regression-based diagnosis of acute st-segment elevation myocardial infarction (stemi) on electrocardiogram (ecg)," *J. Clin. Med.*, vol. 11, no. 18, p. 5408, 2022.

[16] B. J. Kenny and K. N. Brown, "ECG T Wave," 2019.

[17] S. Mawri *et al.*, "The comparison of physician to computer interpreted electrocardiograms on ST-elevation myocardial infarction door-to-balloon times," *Crit. Pathw. Cardiol.*, vol. 15, no. 1, pp. 22–25, 2016.

[18] Y. LeCun, Y. Bengio, and G. Hinton, "Deep learning," *Nat. Methods*, vol. 13, no. 1, p. 35, 2015, doi: 10.1038/nmeth.3707.

[19] J. Wu, X.-Y. Chen, H. Zhang, L.-D. Xiong, H. Lei, and S.-H. Deng, "Hyperparameter optimization for machine learning models based on Bayesian optimization," *J. Electron. Sci. Technol.*, vol. 17, no. 1, pp. 26–40, 2019.

[20] A. Javeed, S. Zhou, L. Yongjian, I. Qasim, A. Noor, and R. Nour, "An Intelligent Learning System Based on Random Search Algorithm and Optimized Random Forest Model for Improved Heart Disease Detection," *IEEE Access*, vol. 7, 2019, doi: 10.1109/ACCESS.2019.2952107.

[21] W. Liu and J. Wang, "Recursive elimination–election algorithms for wrapper feature selection," *Appl. Soft Comput.*, vol. 113, 2021, doi: 10.1016/j.asoc.2021.107956.

[22] R. Garnett, *Bayesian optimization*. Cambridge University Press, 2023.

[23] A. H. Victoria and G. Maragatham, "Automatic tuning of hyperparameters using Bayesian optimization," *Evol. Syst.*, vol. 12, pp. 217–223, 2021.

[24] J. Snoek, H. Larochelle, and R. P. Adams, "Practical bayesian optimization of machine learning algorithms," *Adv. Neural Inf. Process. Syst.*, vol. 25, 2012.

[25] A. I. Kalyakulina *et al.*, "Ludb: a new open-access validation tool for electrocardiogram delineation algorithms," *IEEE Access*, vol. 8, pp. 186181–186190, 2020.

[26] H. Khorrami and M. Moavenian, "A comparative study of DWT, CWT and DCT transformations in ECG arrhythmias classification," *Expert Syst. Appl.*, vol. 37, no. 8, pp. 5751–5757, 2010.

[27] K. Daqrouq, "ECG baseline wandering reduction using discrete wavelet transform," *Asian J. Inf. Technol.*, vol. 4, no. 11, pp. 989–995, 2005.

[28] W. Jenkal, R. Latif, A. Toumanari, A. Dliou, O. El B'charri, and F. M. R. Maoulainine, "An efficient algorithm of ECG signal denoising using the adaptive dual threshold filter and the discrete wavelet transform," *Biocybern. Biomed. Eng.*, vol. 36, no. 3, pp. 499–508, 2016.

[29] M. M. Suhail and T. A. Razak, "Cardiac disease detection from ECG signal using discrete wavelet transform with machine learning method," *Diabetes Res. Clin. Pract.*, vol. 187, p. 109852, 2022.

[30] M. Aqil, A. Jbari, and A. Bourouhou, "ECG Signal Denoising by Discrete Wavelet Transform.," *Int. J. Online Eng.*, vol. 13, no. 9, 2017, doi: 10.3991/ijoe.v13i09.7159.

[31] H. Alibrahim and S. A. Ludwig, "Hyperparameter optimization: Comparing genetic algorithm against grid search and bayesian optimization," in *2021 IEEE Congress on Evolutionary Computation (CEC)*, 2021, pp. 1551–1559.

[32] J. Wang, J. Xu, and X. Wang, "Combination of hyperband and Bayesian optimization for hyperparameter optimization in deep learning," *arXiv Prepr. arXiv1801.01596*, 2018.